A two-step sensitivity analysis for hydrological signatures in Jinhua River Basin, East China

Journal:	*Hydrological Sciences Journal*
Manuscript ID	HSJ-2016-0405.R2
Manuscript Type:	Original Article
Date Submitted by the Author:	n/a
Complete List of Authors:	Pan, Suli; Zhejiang University, Guangtao, Fu; University of Exeter Chiang, Yen-Ming ; Zhejiang University, Department of Hydraulic Engineering Ran, Qihua; Zhejiang University Xu, Yueping; Zhejiang University, Hydraulic Engineering
Keywords:	sensitivity analysis, ANOVA method, Sobol's method, Hydrological signature, DHSVM, Peak flow

Title: A two-step sensitivity analysis for hydrological signatures in Jinhua River Basin, East China

1. Author name and affiliations:

Suli Pan[a], Guangtao Fu[b], Yen-Ming Chiang[a], Qihua Ran[a] and Yue-Ping Xu[a]

[a] Institute of Hydrology and Water Resources, College of Civil Engineering and Architecture, Zhejiang University, Hangzhou, 310058, China

[b] Center for Water Systems, College of Engineering, Mathematics and Physical Sciences, University of Exeter, North Park Road, Harrison Building, Exeter, EX4 4QF, UK

Full postal address and e-mail address:

Suli Pan:

Postal address: Room B526, Anzhong Building, Campus Zijingang, Zhejiang University, No.388 Yuhangtang Road, Hangzhou, China. **E-mail:** pansuli@zju.edu.cn

Guangtao Fu:

Postal address: Center for Water Systems, College of Engineering, Mathematics and Physical Sciences, University of Exeter, North Park Road, Harrison Building, Exeter, EX4,4QF,UK. E-mail: G.Fu@exeter.ac.uk

Yen-Ming Chiang:

Postal address: Room B528, Anzhong Building, Campus Zijingang, Zhejiang University, No.388 Yuhangtang Road, Hangzhou, China. **E-mail:** chiangym@zju.edu.cn

Qihua Ran:

Postal address: Room B519, Anzhong Building, Campus Zijingang, Zhejiang University, No.388 Yuhangtang Road, Hangzhou, China. **E-mail:** ranqihua@zju.edu.cn

Yue-Ping Xu:

Postal address: Room B513, Anzhong Building, Campus Zijingang, Zhejiang University, No.388 Yuhangtang Road, Hangzhou, China. **E-mail:** yuepingxu@zju.edu.cn

2. Corresponding author:

Yue-Ping Xu

Tel.:+86 15924171902. *E-mail address*: yuepingxu@zju.edu.cn (Y-P Xu).

Postal address: Room B513, Anzhong Building, Campus Zijingang, Zhejiang University, No.388 Yuhangtang Road, Hangzhou, China.

The research was conducted at Zhejiang University.

A two-step sensitivity analysis for hydrological signatures in Jinhua River Basin, East China

Suli Pan[a], Guangtao Fu[b], Yen-Ming Chiang[a], Qihua Ran[a] and Yue-Ping Xu [a,*]

[a] Institute of Hydrology and Water Resources, College of Civil Engineering and Architecture, Zhejiang University, Hangzhou, 310058, China

[b] Center for Water Systems, College of Engineering, Mathematics and Physical Sciences, University of Exeter, North Park Road, Harrison Building, Exeter, EX4 4QF, UK

Abstract

Parameter calibration and sensitivity analysis are usually not straightforward tasks for distributed hydrological models, owing to the complexity of model and large number of parameters. A two-step sensitivity analysis approach is proposed for analyzing the hydrological signatures based on the Distributed Hydrology-Soil-Vegetation Model in Jinhua River Basin, East China. A preliminary sensitivity analysis is conducted to obtain influential parameters via Analysis of Variance. These parameters are further analyzed through a variance-based global sensitivity analysis method to achieve robust rankings and parameter contributions. Parallel computing is designed to reduce computational burden. The results reveal that only a few parameters are significantly sensitive and the interactions between parameters could not be ignored. When analyzing hydrological signatures, it is found that water yield was simulated very well for most samples. Small and medium floods are simulated very well while slight underestimations happen to large floods.

* Corresponding author at: Institute of Hydrology and Water Resource, College of Civil Engineering and Architecture, Zhejiang University, room B513, Anzhong Building, No.388 Yuhangtang Road, Hangzhou 310058, China.

Tel.:+86 15924171902. *E-mail address*: yuepingxu@zju.edu.cn (Y-P Xu).

Key words: Sensitivity analysis, ANOVA method, Sobol's method, Hydrological signature, DHSVM, Peak flow

1 Introduction

Distributed physically-based hydrological models have obtained ever-growing attention in recent decades owing to consideration of spatial variability and widely applications for ungauged basins (Razavi and Coulibaly 2012, Zhan *et al.* 2013, Palanisamy and Workman 2014, Noori *et al.* 2014, Noori and Kalin 2016). Applications of these models are wide, including impact analysis of climate change and land cover, runoff and flood forecasting, and improving insights of hydrological process (Du *et al.* 2012, Rahman *et al.* 2013, Xu *et al.* 2013, Tan *et al.* 2015, Winchell *et al.* 2015, Cao *et al.* 2016, Chen *et al.* 2016).

However, the applications of distributed hydrological models for these fields depend on the performance of model simulation, which is optimized by model calibration (Bittelli *et al.* 2010, Cibin *et al.* 2010). Hydrological models are characterized by a set of parameters, varying from simple lumped rainfall-runoff models with several parameters to sophisticated, distributed models with large numbers of parameters, even hundreds (Moradkhani and Sorooshian 2008). Therefore, manual calibration for distributed hydrological models with all parameters is time consuming and practically difficult to find optimal parameter sets. Likewise, a lack of identification for influential parameters in model simulation may cause waste of time on un-influential parameters (Bahremand and De Smedt 2008). Hence, it is very essential to identify the dominant parameters controlling model behavior, which contributes to raising calibration efficiency and obtaining more satisfactory simulation. One useful approach of dominant parameter identification is through implementation of sensitivity analysis (SA), which can quantify the influence of parameters on model response (Wagener *et al.* 2001, Xu and Mynett 2006, Tang *et al.* 2007b, Zhang *et al.* 2013, Zhan *et al.* 2013, Song *et al.* 2015, Ren *et al.* 2016). The results of sensitivity analysis are helpful to determine sensitive parameters which should be paid more attention to in model calibration. A comprehensive comparison of various sensitivity analysis methods are implemented in literatures (Saltelli *et al.* 2000b, Saltelli *et al.* 2004, Tang *et al.* 2007b) and the results reveal that the Sobol's method is the effective method to obtain global parameter sensitivities. Furthermore, Tang *et al.* (2007a) applied the Sobol's method to a distributed hydrological model and obtained robust sensitivity rankings of the parameters, which could be able to significantly reduce the number of parameters for calibrating a hydrological model.

Hydrological signatures are often used to quantify hydrological input variables and response variables (Yadav *et al.* 2007, Westerberg and McMillan 2015). Signatures are widely used for catchment classification (Wagener *et al.* 2007, Sawicz *et al.* 2011), change detection (Archer and Newson 2002) and model calibration (Gupta *et al.* 2008). Yadav *et al.* (2007) adopted hydrological signatures (slope of the flow duration curve (FDC) and runoff ratio) and similarity indices for catchments classification. Hartmann *et al.* (2013a, 2013b) evaluated hydrological model performance with respect to hydrological signatures. Likewise, Westerberg *et al.* (2011) applied several points selected on FDC for model calibration and two selection methods are compared to estimate their impacts on parameter calibration. Furthermore, the application of hydrological signatures in hydrological modeling can offer meaningful information contained in hydrographs. Signatures could also help to interpret the relations between models and underlying hydrological processes and reflect various aspects of model behaviors.

The Distributed Hydrology-Soil-Vegetation Model (DHSVM) (Wigmosta *et al.* 1994), a fully distributed hydrological model, is characterized by numerous parameters. It does not contain any sensitivity analysis or model calibration module. Therefore sensitivity analyses for DHSVM are often implemented using one-factor-at-a-time (OFAT) (Cuo *et al.* 2011), a local sensitivity test using stepwise, single parameter perturbation method (Du *et al.* 2014) and method of Morris (Kelleher *et al.* 2015). These SA methods are all simple or local and could not fully represent the relations between input parameters and model outputs due to their few sample sizes for lots of parameters and the interactions among parameters are often ignored. In this study, a two-step approach is therefore proposed for in-depth sensitivity analysis for DHSVM by adding two SA modules (Sobol's and Analysis of Variance (ANOVA) methods, and iterated fractional factorial design (IFFD) sampling approach is applied in ANOVA to reduce the computational burden) into the DHSVM model, which can provide robust sensitivity rankings and parameter's individual contributions, total contributions and interactions. Additionally, the parameters values for different soil and vegetation types are distinct in this study. In order to fully evaluate the performance of DHSVM, several hydrological signatures are selected in this study.

The structure of this paper is as follows. Section 2 describes the material and methods used in the study. Section 3 presents the results of two-step sensitivity analysis and analysis of hydrological signatures. Section 4 provides discussion concerning the two-step sensitivity analysis approaches and its further application in future. Section 5 summarizes the findings in this study.

2 Material and methods

2.1 Methodology framework

The methodology framework of this study is presented in Figure 1. The first step is to prepare input data for the hydrological model and determine ranges of nearly all parameters. ANOVA sensitivity analysis is then undertaken to obtain preliminary sensitive parameters in the first step. This is because that model outputs are assumed to be normally distributed. Substantial departures from the assumption of normality can affect sensitivity analysis results (Lindman, 1974) and the results of ANOVA sensitivity analysis may not be robust. Therefore, only the effect of individual parameters is adopted in the study. Additionally, the number of model runs in ANOVA method is smaller than that in the Sobol's method used in the second step. These preliminary sensitive parameters from ANOVA are further analyzed via Sobol's method to achieve robust results, including effects of individual parameters and interactions between parameters. Afterwards, final sensitive parameters and their interactions are quantified and ranked. The third step is to interpret the impact of final sensitive parameters on model simulation through considering objective functions, sensitivity index and values of parameters. The fourth step is to execute hydrological signature analysis and percentile analysis for peak flows for samples with efficiency criteria > 0.7. Moreover, detailed signatures analysis and percentile analysis are done for selected individual samples.

Figure 1. Methodology framework used in this study.

2.2 Study area

Jinhua River, a tributary of Qiantang River, is located in the Midwest of Zhejiang Province, East China (Figure 2). This river has a length of 195 km and the catchment area is 6 782 km^2 (Xu *et al.* 2015). In this study, the basin above Jinhua hydrological station is included and its catchment area is 5 996 km^2, which is appropriate to apply DHSVM model (the model is mainly applicable to watersheds whose area is less than 10 000 km^2). Also this model has been successfully used in the study area (Xu *et al*. 2015). The prevailing climate of the basin is Asian subtropical monsoon, which is characterized by abundant precipitation and high temperature in summer and rainless and cold winter. The annual average temperature is 17 ℃. The elevation ranges from 29 to 1 296 m in the basin (Figure 3). The annual mean precipitation is 1 424 mm. More than 50% of the annual total precipitation happens in the period from May to July. Because of the unevenly temporal distribution of precipitation, Jinhua River Basin suffers a lot from droughts and floods. Good hydrological simulation will provide support to disaster prediction and prevention, and sustainable river management. Figure 2 also presents the locations of five meteorological stations and the hydrological station used in the study.

Figure 2. Location of the six stations used in the study.

2.3 Overview of DHSVM

Distributed Hydrology-Soil-Vegetation Model (DHSVM) (Wigmosta *et al.* 1994, Wigmosta and Burges 1997, Wigmosta *et al.* 2002) is a physically-based distributed hydrological model. DHSVM provides an integrated representation of hydrology-vegetation dynamics at the spatial scale identified by digital elevation map (DEM) data (the spatial resolution is typically 10-200 m). The river basin is separated into computational grid cells depending on DEM. Soil and vegetation characteristics are allocated to each computational grid cell. At each time step, DHSVM offers simultaneous solution to water and energy balance equations for every grid cell in the river basin. The hydrological connection of individual grid cell is realized by surface and subsurface flow routing. The spatial and temporal resolutions are 200 m and daily respectively. The version 3.1.1 of DHSVM is adopted in this study.

DHSVM consists of seven modules, i.e., evapotranspiration, snowpack accumulation and melt, canopy snow interception and release, unsaturated moisture movement, saturated subsurface flow, surface overland flow and channel flow (Wigmosta *et al.* 2002). Evapotranspiration is presented adopting a two-layer canopy model with both two layers divided into wet and dry areas. Modules concerning snow, i.e., snowpack accumulation and melt and canopy snow interception and release, are not considered here owing to the fact that snow is rare in the study area. Unsaturated moisture movement with multiple root zone soil layers is assessed utilizing Darcy's Law (Domenico and Schwartz 1988). Every grid cell exchanges available water with its adjacent grid cells using a function of its hydraulic conditions bringing about a transient, three-dimensional formulation of saturated subsurface flow and surface flow. DHSVM adopts a cell-by-cell method to route saturated subsurface flow utilizing a kinematic or diffusion approximation (Wigmosta *et al.* 1994, Wigmosta and Lettenmaier 1999). Grid cells in the basin are centered on each DEM point.

Surface runoff is routed by a unit hydrograph method or an explicit cell-by-cell method (the explicit cell-by-cell approach is adopted in this study). Surface runoff occurs in a cell when meeting any of the following conditions: firstly, the available water in grid cell exceeds the defined infiltration capacity; secondly, the water table exceeds the ground surface. The downslope movement of surface runoff is based on a cell-by-cell mode which is similar to the approach applied for subsurface flow. Flow in stream channels and road drainage ditches is routed by utilizing a cascade of linear channel reservoirs. Roads are not considered in this study owing to the fact that detailed road information is not available and the area percentage of roads is very small compared to the big basin area. However, it is kept in the mind that roads often generate overland flow from compacted surfaces, intercept subsurface flow at road cuts and alter hillslope hydrologic processes. Ignoring the roads may affect the accuracy of hydrological simulation, in particular peak and peak time. In the model, lateral inflow to a channel segment, from the cells which it passes through, is composed of subsurface flow and overland flow intercepted by channels.

Generally, DHSVM parameters can be classified into elevation, stream, road, soil and vegetation categories. Parameters related to the characteristics of stream network such as stream segment length, width and aspect are determined based on the DEM data. That is to say, these parameters do not need to be calibrated. Soil/vegetation parameters such as field capacity need to be calibrated if its real value in physical meaning is not known or no observation is available. The calibration of vegetation and soil parameters in DHSVM is very common in other studies (Thanapakpawin *et al.* 2007, Safeeq and Fares 2012, Cuartas *et al.* 2012).

2.4 Model input data

The climate data including average air temperature, wind speed, relative humidity, sunshine duration and precipitation from five meteorological stations, i.e., Jinhua, Dongyang, Wuyi, Yongkang and Yiwu (Figure 2), are available in this study. The climate data is obtained from Zhejiang Provincial Metrological Administration. The incoming shortwave radiation and longwave radiation are calculated using climate data. The observed runoff at Jinhua hydrological station is obtained from Zhejiang Provincial Hydrology Bureau (Figure 2). The time period of climate and runoff data is from 1991-2000.

The other data needed for DHSVM include watershed boundary (mask), digital elevation map (DEM), soil type, vegetation type, soil depth and streams network. The DEM data (Figure 3) with a resolution of 90 m are downloaded from the Shuttle Radar Topography Mission (SRTM) website (http://srtm.csi.cgiar.org/). Considering computational burden, the resolution of DEM is redefined to 200 m in the model. The water boundary is determined based on DEM. The soil data (Figure 3) are obtained from Nanjing Institute of Soil Research, China. According to the USDA (United States Department of Agriculture) soil texture classification system needed in DHSVM, the soil classes are reclassified. The vegetation data (Figure 3) are obtained from WESTDC Land Cover Products 2.0 (2006) (http://westdc.westgis.ac.cn). Table 1 shows vegetation and soil classes and their percentages in Jinhua River Basin. The soil depth and streams network are generated based on DEM and mask using Arc Workstation.

Figure 3. DEM (digital elevation map) (a) soil distribution (b) and vegetation distribution (c) in Jinhua River Basin.

Table 1. Vegetation and soil classes and their percentages in Jinhua River Basin.

2.5 Analysis of Variance (ANOVA) sensitivity analysis

For this study, Analysis of Variance (ANOVA) is adopted to determine the preliminary sensitive parameters in DHSVM simulation owing to its popularity and common application (Steel

229 and Torrie 1988, Shinohara *et al.* 2016). In this method, parameters are sorted into specific scope of
230 parameter values indicating intervals with same parameter value width. Based on ANOVA
231 terminology, inputs are referred to as "factor" and values of factors are referred to as factor levels.
232 Moreover, output is called "response variable". ANOVA method was proposed by Fisher (1925).
233 The F value is a key statistic in ANOVA and describes the statistical significance of differences in
234 the mean responses among the levels of corresponding parameter. Therefore, the F values are
235 utilized to judge whether parameter causes difference in response variable, i.e. sensitivity. The
236 higher the F value is, the more crucial parameter is. Then, the parameter is more sensitive in
237 model simulation. The equation of F value is described as follows:

238 $$F = \frac{\bar{S}_A}{\bar{S}_E} \quad (1)$$

239 Where $\bar{S}_A$ is referred to group (treatment) mean squares from factor A, which reflects the
240 differences between mean value of samples in different levels and mean value of all samples. $\bar{S}_E$
241 is referred to error (residual) mean squares, which reflects the differences between value of each
242 sample and mean value of samples in different levels.

243 One-way ANOVA is used to evaluate the significance of one factor on response variable.
244 Two-way ANOVA is dealt with two or multiple factors and applied to determine the single effect
245 of factor and interaction effects between factors. No assumption is demanded regarding the
246 functional form of relationships between the outputs and the inputs in ANOVA. Generally,
247 ANOVA method could apportion the variance, but substantial departures from the assumption of
248 normality can affect analysis results (Lindman, 1974). Therefore, only the effect of individual
249 parameter is adopted in the study.

250 ANOVA will become computationally infeasible if the number of input is large. The number

251 of model runs could be decreased and computational efficiency will be much higher by using IFFD sampling approach (Saltelli *et al.* 1995, Andres 1997). In IFFD, parameters are sampled at three different levels (groups): low, middle and high, rather than from a continuous range (Saltelli *et al.* 1995). These discrete levels are defined equally within the original parameter scope. The use of a slight number of factor levels empowers the sampling formula to achieve results effectively and accurately (Andres 1997). In Jinhua River Basin, there are ten vegetation classes and six soil classes. The number of parameters is more than 200, if all soil and vegetation classes are included. Because there is hardly any snow in the study area, parameters concerning snow are excluded in sensitivity analysis. Moreover, soil and vegetation classes are only chosen when their area percentages in the basin are higher than 10%. Thus, the vegetation and soil classes in italic script in Table 1 are selected. In total, three soil classes, i.e., sandy loam (SL), loam (L) and clay loam (CL), and three vegetation classes, i.e., mixed forests (MF), grasslands (GL) and cropland (CrL) are finally considered in ANOVA sensitivity analysis. The total percentages for selected soil and vegetation classes are about 90%. Consequently, in ANOVA sensitivity test, the number of parameters is 83 and the sample size is 14 000. According to Cuo *et al.* (2011), model simulation is sensitive to both vegetation height and vegetation minimum resistance. Different parameter ranges are used for these vegetation parameters in different vegetation stories (as shown in Table 2, italic). Ranges, unit and abbreviation of selected parameters are presented in Table 2. Besides, monthly LAI in different months is distinguished via appropriate multipliers and the ranges of LAI in Table 2 are represented for January which has the minimum LAI.

Table 2. Ranges, unit and abbreviation of constant, soil and vegetation parameters for ANOVA sensitivity analysis.

2.6 Sobol's sensitivity analysis

Sobol's sensitivity analysis method (Saltelli *et al.* 2000a, Sobol' 2001), a variance-based method, is selected in this study for in-depth global sensitivity analysis since this method is able to quantify not only the contributions of individual parameter to DHSVM simulation but also their interactions, which could not be obtained accurately from ANOVA (Zhang *et al.* 2013, Xu *et al.* 2014). In addition, sensitivity index provided by the Sobol's method are more effective than other sensitivity analysis methods for its capability of describing the interactions between a large number of variables for extremely nonlinear models, such as distributed hydrological models (Tang *et al.* 2007a, Tang *et al.* 2007b, Rajabi *et al.* 2015). In this method, the attribution of total output variance to individual model parameters and their interactions can be defined as follows (Bois *et al.* 2008):

$$V = \sum_{i}(V_i) + \sum_{i<j}(V_{ij}) + \sum_{i<j<m}(V_{ijm}) + \cdots + (V_{1,2,\ldots,k}) \tag{2}$$

Where V is the total variance of model output; V_i is the first order variance for the ith variable x_i; V_{ij} is the interaction variance between x_i and x_j; k is the total number of input variables. The variances displayed in Equation (2) can be assessed by approximate Monte Carlo numerical integrations. The sensitivity of individual parameters or their interactions, i.e.sensitivity index are calculated according to their contribution in the total variance V.

First order sensitivity index $S_i = \dfrac{V_i}{V}$ (3)

Second order sensitivity index $S_{ij} = \dfrac{V_{ij}}{V}$ (4)

Total order sensitivity index $S_{Ti} = \dfrac{\sum_{i}(V_i) + \sum_{i<j}(V_{ij}) + \sum_{i<j<m}(V_{ijm}) + \cdots + (V_{1,2,\ldots,k})}{V}$ (5)

Where S_i is the first order sensitivity index corresponding to the input factor x_i; the second order sensitivity index S_{ij} evaluates the interactions between x_i and x_j; the total order sensitivity index S_{Ti} calculates the total effects of the input factor x_i on the model simulation.

2.7 Objective function and parallel computing

The proper choice of an objective function is often demanded for evaluating the performance of a hydrological model in sensitivity analyses and model calibration, but not essential (Hartmann *et al*. 2015, Pianosi *et al*. 2016). Objective function must be able to accurately express the distance between observation and simulation. Comprehensive objective functions and efficiency criteria have been used in hydrological simulation (Rao and Han 1987, Yan and Haan 1991). In the study, Nash-Sutcliffe efficiency (*NS*) is firstly selected. *NS* is a normalized statistic that confirms the relative difference of residual variance in contrast to observation variance (Nash and Sutcliffe, 1970). *NS* is calculated as shown in Equation (6). *NS* is more sensitive to peak flows than low flows because squared deviations is utilized which leads to the possibility that low flows is not accurately simulated by hydrological models (Schaefli and Gupta 2007, Criss and Winston 2008, Muleta 2012, Hartmann *et al.* 2015). E_{rel} (Equation (7)) is a statistic which is widely applied to evaluate the performance of low flow simulation (Krause *et al.* 2005, Raposo *et al.* 2012). The combination with equal weights (*NE*; Equation (8)) is then used as the final objective function in this study. The relevant equations are shown as follows:

$$NS = 1 - \frac{\sum_{i=1}^{n}(O_i - S_i)^2}{\sum_{i=1}^{n}\left(O_i - \overline{O}\right)^2} \tag{6}$$

$$E_{rel} = 1 - \frac{\sum_{i=1}^{n}\left(\frac{O_i - S_i}{O_i}\right)^2}{\sum_{i=1}^{n}\left(\frac{O_i - \overline{O}}{\overline{O}}\right)^2} \tag{7}$$

$$NE = 0.5 \times NS + 0.5 \times E_{rel} \tag{8}$$

Where O_i is referred as the observed streamflow; S_i is referred as the simulated streamflow; $\overline{O}$ is referred as the average of observed streamflow.

DHSVM runs relatively slowly. The meteorological data used in this study are from 1991 to 2000 at daily scale data. The cell grid is 200m and the basin area is 5 996 km^2. Therefore, each run of model will take about 50 minutes under Linux server. The run time of DHSVM is 486 days in ANOVA sensitivity analysis with a sample size of 14 000. Similarly, the run time is 708 days in Sobol's sensitivity analysis with a set of 20 400 samples. Computer cluster consisting of five PCs with same configurations is used in this study and the logistical setup of computer cluster is a master-slave distribution. In other words, one PC plays as master and assigns tasks to slaves, i.e., the other four PCs. The slaves receive and finish the tasks from the master. Moreover, in order to decrease the run interval, the master also participates in running task as well as slaves. And the configuration in PC is single-CPU (central processing unit) with four cores. Moreover, Hyper-Threading (with Hyper-Threading, one physical core appears as two processors to the operating system) is installed in five PCs and the number of processors is then forty. The softwares which are necessary to be set up in five PCs include gcc, g++, NFS (File Share System), SSH (Secure Shell) and MPI (Message Passing Interface). The parallel pattern in this study is data-parallel. That is to say, the tasks for slaves and master are running model based on the sample sets generated by sensitivity analysis methods, and the process of generating sample sets is done on the master. The run intervals of ANOVA and Sobol's sensitivity analyses are 13 days and 18 days respectively via parallel computing. The computational efficiency has been greatly enhanced after parallel computing.

2.8 Hydrological signatures

Hydrological signatures are able to investigate the simulation effect of hydrological models more comprehensively and thoroughly (Yadav *et al.* 2007, Yilmaz *et al.* 2008, Winsemius *et al.* 2009). To analyze the performance of different aspects of streamflow simulated via DHSVM, five distinct conditions of hydrological signatures are selected, including average flow conditions, low flow conditions, peak flow conditions, duration of flow events for low flow conditions and duration of flow events for peak flow conditions (Olden and Poff 2003, Bormann *et al.* 2011, Westerberg and McMillan 2015, Shafii and Tolson 2015). The specific hydrological signatures of different conditions are described in Table 3, i.e., mean annual runoff for average flow conditions, low flow signature and base-flow signature for low flow conditions, specific mean annual maximum flows for peak flow conditions, annual minimum of 1-/3-/7-/30-d means of daily runoff and annual maximum of 1-/3-/7-/30-d means of daily runoff for duration of flow events. The detailed abbreviation, unit and definition are shown in Table 3.

Table 3. Description of the six hydrological signatures used in the study.

In order to evaluate the performance of simulation results conveniently, a new criterion (P) is used and can be calculated by Equation (9). The value of hydrological signatures for observed streamflow is constant. However, P-value of simulated streamflow changes depends on each parameter set.

$$P = \frac{HS(Q_{\mathrm{sim}})}{HS(Q_{obs})} - 1 \tag{9}$$

Where $HS(Q_{\mathrm{obs}})$ is referred as the value of hydrological signature for observed streamflow; $HS(Q_{\mathrm{sim}})$ is referred as the value of hydrological signature for simulated streamflow.

As shown in Equation (9), if P>0, the value of hydrological signature for simulated streamflow is higher than that of observed streamflow, indicating that the simulated signature is overestimated. On the contrary, the simulated signature is underestimated. The lower the absolute value of *P* is, the higher performance of hydrological model is.

As described in Section 2.1, Jinhua River Basin suffers a lot from floods. Besides the peak-related hydrological signature shown in Table 3, peak flows extracted from observed and simulated runoff are compared via percentiles. Here, Peak-over-threshold (POT) (Obrien *et al.* 2015, Hirsch and Archfield 2015, Mallakpour and Villarini 2015) is adopted to select peak flows. For POT method, the choice of the threshold is important. If the threshold is too low, excessive number of peak flows is selected. On contrary, only a few peak flows are considered when the threshold is too high. In this study, mean of observed daily runoff (1991-2000) is used. Two subsequent peak events (P_1 and P_2) are identified as independent when the following two conditions are satisfied (Lang *et al*. 1999):

$$\begin{cases} \theta > 5 + \log(Area) \\ X_{\min} < \left(3/4\right)\min(P_1, P_2) \end{cases} \tag{10}$$

Where θ is the interval of two subsequent peak events (days); $Area$ is the area of watershed (miles^2); $X_{\min}$ is the minimum runoff during interval of two subsequent peak events (m^3/s).

Based on these independent conditions and selected threshold, peak flows are extracted from the observed and simulated runoff in the study period (1991-2000).

3 Results

3.1 ANOVA sensitivity analysis result

Figure 4 presents the *F*-value and percentage of the total variance at a significance level of $p=0.05$. Sixteen sensitive parameters are preliminarily selected from all parameters (83) of DHSVM, based on the criterion that *F*-Value is bigger than 3.0. The sum of variance percentages of selected sixteen parameters is about 97.6%. The higher the *F*-value is, the more sensitive the parameter is.

Figure 4 shows that *F*-values of some parameters exceed three orders of magnitude larger than 3.0. Hence, a threshold of 300 is adopted to determine whether a parameter is highly sensitive or not. There are three highly sensitive parameters, i.e., rain LAI multiplier (*Rj*), porosity of clay loam ($\varphi(CL)$) and field capacity of clay loam ($\theta fc(CL)$), accounting for 19.3%, 9.6% and 40% of total variance respectively. Among these highly sensitive parameters, field capacity of clay loam is the most sensitive parameter and its *F*-value is 1 583.4 which is far larger than the threshold 300. Field capacity together with root zone depth *(D(CrL))* determines realistic storage of available water in soil, and realistic storage will diminish with the decrease of field capacity. Consequently, the same amount water access soil subsurface layers will have higher runoff with decreasing field capacity. However, porosity together with root zone depth decides the capacity of water in soil. Simulated peak flows will decrease and routing time will increase with increasing porosity. Rain LAI multiplier is LAI multiplier for rain interception, which will influence interception storage and evaporation.

Thirteen sensitive parameters are presented in Figure 4, including five soil parameters (mainly from clay loam) and eight vegetation parameters (related to mixed forests and croplands). Understory minimum resistance *(URsmin(MF))* and overstory minimum resistance *(ORsmin(MF))* of mixed forest are sensitive parameters. According to Wigmosta *et al.* (2002), canopy resistance is calculated separately for the understory and overstory. Similarly, understory height *(Uh(MF))* of mixed forest is sensitive to simulated streamflow. Additionally, in reality, the actual values for understory and overstory height of mixed forest are different. Vegetation height is related to aerodynamic resistance, which determines the rate of potential evaporation with other parameters. Vegetation minimum resistance, vapor pressure deficit *(Ec(CrL))* and soil moisture threshold *(θ*(CrL))* are used to calculate canopy resistance, which directly impact vegetation transpiration. LAI affects the capacity of canopy interception and acquisition of solar radiation. Therefore, the rate of potential evaporation will increase with increasing LAI. Lateral conductivity *(K(CL))* is used in the calculation of lateral flow movement and lateral conductivity exponential decrease *(f(CL))* describes exponent decrease of lateral conductivity with soil depth. Both of them influence the amount of lateral flow and routing time. Wilting point *(θwp(CL), θwp(L))* and bulk density *(ρB(CL))* are related to soil evaporation.

Figure 4. ANOVA parameter sensitivities based on the *NE* measure (*F*-value > 3).

Figure 5 shows the observed and simulated hydrographs (when the value of *NE* is the maximum in ANOVA sensitivity analysis) of 1994, 1995 and 1996, which correspond to moderate, wet and dry year respectively. The efficiency criteria for *NS*, E_{rel} and *NE* (1991-2000 years) are 0.83, 0.81 and 0.82 respectively, which show a good performance of the hydrological model. In addition, the bias is -7.8%, which is well within the range -25%~25% (Safeeq and Fares 2012, Xu *et al.* 2015). However, the runoff, especially peak flow, is slightly underestimated.

418 In general, the simulation demonstrates that DHSVM is able to simulate river flows in a good way. Also it can be observed from Figure 5 that the model performance in the dry year (1996) is better than that in the moderate year (1994).

Figure 5. Model performance in 1994, 1995 and 1996 (corresponding to moderate, wet and dry year, respectively) when the value of *NE* (*NS*, E_{rel} and *NE* are 0.83, 0.81 and 0.82 respectively) is the maximum in ANOVA sensitivity analysis.

3.2 Sobol's sensitivity analysis results

The input factors for Sobol's sensitivity test are preliminary sensitive parameters selected by ANOVA (as shown in Figure 4 and Table 4). As shown in Table 4, sixteen model parameters are considered in Sobol's sensitivity analysis and a sample size of 20 400 is used (according to Saltelli and Tarantola (2002), this sample size is appropriate). Saltelli (2000a) extended the Sobol's original work by adding special transformation to the randomly sampled parameters to reduce computational complexity. This transformation is used in this study and the ranges of porosity, field capacity and wilting point of clay loam are slightly changed (Italic in Table 4). The value of *NE* ranges from 0.2 to 0.88. Percentage of samples with *NE* value higher than 0.8, is up to 66.7%. Percentage of E_{rel} that is larger than 0.8 accounts for nearly 60% and the highest value of E_{rel} is 0.93. Moreover, a majority of samples has a value of *NS* higher than 0.7. In addition, biases are also calculated for all samples, and nearly all values are within the acceptable range of -25%~25% (Safeeq and Fares 2012). The percentage of correlation coefficient value higher than 0.9 is nearly 97%.

The total order sensitivity index is shown in Figure 6. Total order sensitivity index of 16 parameters range from 0.00 to 0.29. According to Tang *et al.* (2007b), parameters are highly sensitive when the sensitivity indices are higher than 0.1 and sensitive with the indices higher than 0.01. Parameters are insensitive to streamflow simulation when its total order sensitivity index is smaller than 0.01. Figure 6 shows that there are eight highly sensitive parameters, including one constant parameter (rain LAI multiplier), four soil parameters (lateral conductivity, porosity, field capacity and wilting point of clay loam), and three vegetation parameters (understory monthly LAI, understory minimum resistance and root zone depths of croplands). Compared with the results from ANOVA sensitivity test, it shows that the identified parameters are similar and the ranking of them is compatible. Moreover, the most sensitive parameter in both methods is field capacity of clay loam. The role of field capacity (*θfc(CL)*) is dominant in unsaturated moisture movement module. In DHSVM model, no unsaturated flow is allowed to occur when the moisture content is below the field capacity. Unsaturated flow will increase with decrease of field capacity. The amount of runoff is obviously impacted by the value of field capacity. The higher the value of field capacity is, the more runoff will generate. In other words, more runoff could be obtained by decreasing the value of field capacity. Root zone depth (*D(CrL)*) has significant impacts on unsaturated flow, soil evaporation and the amount of moisture in the soil column. Model simulation is also highly sensitive to wilting point (*θwp(CL)*) and understory LAI (*ULAI(CrL)*), owing to the fact that both of them play important roles in canopy resistance and evapotranspiration. As shown in Figure 3 and Table 1, the area percentage of forests/mixed forests is 34.7% (5.0%+0.1%+29.6%), and the area percentage only with understory is 64.5% (1.2%+22.9%+0.4%+36.7%+3.3%). It is easy to overlook that forests/mixed forests also have understory. Additionally, the mixed forest in the study area mainly consists of grasslands, shrublands and trees. The area percentage of trees in the mixed forest is about 30%, or less.

Moreover, the vegetation overstory parameters only have slight impacts on canopy interception and vegetation transpiration. This is an explanation for the conclusion that vegetation parameters related with overstory are less sensitive to model simulation.

Table 4. Ranges, number and abbreviation of parameters for Sobol's sensitivity analysis.

Figure 6. Sobol's total order sensitivity index based on the *NE* measure.

Interactions between parameters, i.e., second order sensitivity index, are presented in Figure 7. These interactions could not be identified with other local sensitivity analysis methods, such as OFAT (One-factor-at-a-time). The x-axis and y-axis are parameter numbers shown in Table 4. The constant parameter, rain LAI multiplier, has interactions with other fifteen parameters as shown in the first column of Figure 7. However, all sensitivity indices are smaller than a threshold value of 0.01, i.e., insensitive interactions. The interactions among field capacity of clay loam and other parameters are important. The second order sensitivity index between field capacity of clay loam and understory monthly LAI of croplands is the maximum and the value reaches 0.03. The total order sensitivity index of field capacity of clay loam reaches 0.29, which is much larger that its first order sensitivity index (0.18). As presented in Figure 3, clay loam and croplands covered most areas of the study area. In DHSVM model, LAI has direct effects on three crucial hydrological processes, i.e., vegetation canopy rainfall interception, evaporation and soil transpiration. LAI affects acquisition of solar radiation and is used as a multiplier in canopy precipitation interception. And the rate of potential evaporation will increase with the increase of LAI and available water into soil will then decrease. Moreover, field capacity is used to determine the realistic storage of available water in soil. Hence, the streamflow simulation is proven to be sensitive to the interactions between these parameters.

In addition, the interactions between field capacity of clay loam and root zone depth of croplands are also sensitive, for the reason that field capacity determines plant available water in soil with root zone depth *(D(CrL))*. The interactions increase the value of total order sensitivity index of root zone depth to 0.27. Similarly, the interactions between field capacity of clay loam and soil moisture threshold of croplands are also sensitive. The total sensitivity index of soil moisture threshold reaches to 0.07, which is much larger than its first order sensitivity index (0.03). This is due to the fact that soil moisture threshold also has an impact on transpiration of soil like LAI. Understory height affects evaporation and transpiration of vegetation. This explains the strong interactions between field capacity and understory height. Likely, the reason for that model simulation is sensitive to the interactions between field capacity and vapor pressure deficit is owing to the fact that vapor pressure deficit has an impact on evaporation and transpiration of vegetation. In addition, vegetation minimum resistance affects water balance and vegetation transpiration. Both wilting point and LAI have a significant influence on evaporation of soil. So their interactions are sensitive to model simulation.

Figure 7. Interactions among sixteen parameters based on the *NE* measure.

3.3 Hydrological signatures

Six representative hydrological signatures from four flow conditions are selected in this study. Evaluation criterion *P*-value shown in Equation (9) is used to analyze the performance of the hydrological model based on hydrological signatures. Figure 8 shows the boxplots of *P*-values for four hydrological signatures of all samples used in Sobol's sensitivity analysis, i.e., mean annual runoff *(A1)*, Low flow signature *(L1)*, Base-flow signature *(L2)* and Specific mean annual maximum flows *(H1)*. For hydrological signature *A1*, *P*-values range from -1.0 to 0.4. However, the *P*-values between 1% and 99% percentiles are totally within the acceptable scope (-25%~25%), which illustrates that the overall performance of *A1* is good. For hydrological signatures *L1*, approximately 96% of *P*-values are bigger than 25%, that is to say, the percentage for *P*-value within the acceptable range is only 4%. A number of samples are good with the *P*-value of *L2* close to zero. All of *P*-values of *H1* are lower than zero and 15.8% of *P*-values of *H1* are within the acceptable scope.

Figure 8. Boxplot for *P*-value of hydrological signatures (A1 (Mean annual runoff), L1 (Low flow signature), L2 (Base-flow signature): and H1 (Specific mean annual maximum flows)) of all samples in Sobol's sensitivity analysis.

In order to better understand the performance of the model concerning the four hydrological signatures in some specific samples, four samples with the value of *NE* higher than 0.7 are selected from all samples in Sobol's sensitivity analysis. Four samples, i.e., *Sample A*, *Sample B*, *Sample C* and *Sample D*, are selected according to the distinct intervals of *NE* value shown in Table 5. *Sample A* has the maximum value of *NE*. The results are displayed in Table 6. For *Sample A*, *P*-value of *A1* is -0.10 and that of *L1*, *L2* and *H1* are 0.68, -0.35 and -0.29 respectively. This explains that a high value of efficiency criteria could not guarantee good performance in all aspects of a hydrograph. For *Sample B,* hydrological signature *L1* (0.07) is close to zero and *A1* (-0.23) also within the acceptable range. *L2* (-0.54) and *H1* (-0.30) indicate less satisfactory simulations of base flow and peak flow. Nevertheless, base flow is reasonably simulated with *L2* (0.09) in *Sample C*, so is mean annual runoff (*A1* is equal to 0.01). For *Sample D*, peak flow is excellently simulated with *H1* (-0.22). Taking the total order sensitivity index (Section 3.2) and corresponding parameter values in *Sample A* into account, high value of porosity (0.58) and field capacity (0.39) in clay loam result in the inferior performance of hydrological signature *L1*, *L2* and *H1*.

Table 5. Selected samples based on the *NE* value.

Table 6. Hydrological signatures of the observed and the simulated from selected samples and corresponding *P*-values.

Other hydrological signatures *DH1-4* and *DL1-4* of four selected samples are displayed in Figure 9 and Figure 10 respectively. For *DH1*, all four samples underestimate annual maximum of 1-day means of daily runoff in 1991-2000. As shown in Figure 9, the ranking of performance in *DH1* is *Sample D* > *Sample A* > *Sample B* > *Sample C*. This ranking is similar to that of hydrological signature *H1*. Underestimation is greatly improved in *DH2*. For *DH3*, four selected samples perform very well in 1991-2000. For *Sample D*, runoff is mostly overestimated with minor degrees in all years in *DH4*, which corresponds to hydrological signature *A1* with 0.21 of *P*-value. Different to *DH1-3*, the ranking of *DH4* is that *Sample C* is the best, *Sample A* is the second, *Sample B* is the third and *Sample D* is the last. And the ranking of *DH4* is similar to that based on hydrological signature *A1*.

Figure 9. Hydrological signature *DH1-4* for observed and simulated runoff from four selected samples as shown in Table 5.

As presented in Figure 10, for *DL1*, *Sample B* simulates very well in all years. However, other three samples underestimate *DL1* during most years. This ranking is totally similar to that of hydrological signature *L1*. The overestimation is improved for four samples in *DL2*. For *DL3*, performance of four samples is further better than *DL1* and *DL2*. By comparing the meaning of *DL3* and *L2*, it is reasonable that the ranking of *DL3* is the same to *L2*. The ranking of *DL4* is similar to that based on hydrological signature *A1*.

Hydrological signatures *DH1-4* and *DL1-4* represent maximum and minimum annual flow of various durations, which describe the performance of duration of flow event in model simulation and provide important insights into a hydrograph. As shown in Figure 9 and Figure 10, the performance of four selected samples in *DH1* and *DL1* is not ideal. However, performance of *DH3* and *DL3* is good, which illustrates annual maximum and minimum of 7-day means of daily runoff are reasonably simulated.

Figure 10. Hydrological signature *DL1-4* for observed and simulated runoff for four selected samples as shown in Table 5.

Besides six hydrological signatures described above, peak flow percentile is further used to explore the performance of peak flow simulation. Figure 11 shows the peak flow percentiles for the observed and selected samples. These samples are from Sobol's sensitivity analysis samples and chosen with *NS* higher than 0.7. As presented in Figure 11, $Q_{s\text{-}1}$ (1^{th} percentile flows) – $Q_{s\text{-}70}$ (70^{th} percentile flows) are simulated reasonably. However, Figure 11 also shows that extreme peak flows (with percentile larger than 0.75）are not well simulated which is corresponding to the performance of hydrological signature *H1* and streamflow curve shown in Figure 5.

Figure 11. Peak flow percentiles for observed and simulated runoff from samples whose *NS* > 0.7 in Sobol's sensitivity analysis.

In order to understand the performance of peak flow simulation in individual samples, three samples are selected based on the *NS* value instead of *NE* value (Considering the fact that the maximum value of *NS* is 0.85 and *NS* should be bigger than 0.7, three not four distinct intervals are identified). Three samples, i.e., *Sample PA* (maximum value of *NS*), *Sample PB* and *Sample PC*, are selected according to various intervals of *NS* value shown in Table 7. The results are shown in Figure 12. For *Sample PA*, $Q_{s\text{-}1}$- $Q_{s\text{-}25}$ is simulated very well. However, the other peak flow percentiles are underestimated in *Sample PA*. The reason for this is the high value of field capacity (0.38) and low value of wilting point (0.07) of clay loam. For *Sample PB*, Q_{s-1}- Q_{s-75} exhibits slight overestimation. *Sample PC* performs better than the others, Q_{s-1}- Q_{s-70} is totally consistent to Q_{o-1}- Q_{o-70} and Q_{o-75} - Q_{s-99} shows less underestimation.

Table 7. Selected samples for peak flow based on the *NS* value.

Figure 12. Peak flow percentiles for observed and simulated runoff from three selected samples as shown in Table 7.

4 Discussion

It is common to apply one sensitivity analysis method to hydrological models and identify dominant parameters in hydrological model simulation. However, the proposed framework in this study provides a means to identify parameter sensitivities of DHSVM by using a two-step sensitivity analysis approach. In the first step, the ANOVA method was used to identify preliminary sensitive parameters in the DHSVM model simulation. This is because model outputs are assumed to be normally distributed, which may cause the results of ANOVA sensitivity analysis not robust. Therefore, only the effect of individual parameters is adopted in the first step. The ANOVA method was actually used here as a screening sensitivity analysis method. Then these preliminary sensitive parameters identified by ANOVA were further analyzed via the Sobol's method to achieve robust results, including effect of individual parameters and interactions between parameters in the second step. In the end, the performance of the model was investigated for different parameter sets based on hydrological signatures. As we explained before, our aim here is to mainly provide parameter identification results for further calibration and validation. However, we believe during this sensitivity analysis stage, checking how the different parameter sets play a role in model simulation (through hydrological signature analysis) can also be interesting.

In the two-step sensitivity analysis approach, the Sobol's method can apportion the variance in model output (streamflow) to the variance in the model parameters and meanwhile consider interactions among parameters. The results demonstrated that field capacity of clay loam is the most important, showing the largest total order sensitivity index and high value of interactions with other parameters. Others sensitive parameters include rain LAI multiplier affecting evaporation, lateral conductivity and porosity of clay loam contributing to streamflow simulation, and wilting point of clay loam affecting soil evaporation. Highly sensitive vegetation parameters consist of understory monthly LAI of croplands influencing evaporation, understory minimum resistance of croplands strongly affecting water balance and root zone depths of croplands influencing soil evaporation. These results are in good agreement with that of Du *et al.* (2014) who showed that vegetation LAI, minimum resistance, porosity, rain LAI multiplier, wilting point and field capacity are important parameters in the simulation of water yield in northern Idaho, USA, using a stepwise, single parameter perturbation method. Cuo *et al.* (2011) also concluded that lateral saturated hydraulic conductivity, porosity, minimum resistance and LAI should be given special attentions during model calibration based on One-factor-at-a-time (OFAT). Meanwhile, other literatures have studied parameters sensitivities of DHSVM to model simulation as well (Surfleet *et al.* 2010, Kelleher *et al.* 2015). Nevertheless, the sensitivity analysis methods used in these studies could only obtain single contribution of parameters or less robust sensitivity results. The Sobol's method is able to achieve robust sensitivity rankings and, what's more, the interactions between parameters. In particular, in the current study, the interactions between field capacity of clay loam and other parameters cannot be ignored. As shown in Figure 6, the total order sensitivity index becomes 0.29, which is much larger than the first order sensitivity index (0.18) after considering the interactions. This study demonstrates that the Sobol's method did provide valuable information to parameter selections in DHSVM calibration, and promote further guides in searching for optimal parameter sets for this model through considering parameter interactions.

In this study, several soil and vegetation types whose area percentages are bigger than 10% were considered in the two-step sensitivity analysis. Simplified soil and vegetation classes in the sensitivity analysis for DHSVM model may have an impact on simulation results (Cuo *et al.* 2011, Surfleet *et al.* 2010, Du *et al.* 2014). For instance, it is obvious that model simulation will be affected if same values were set for overstory vegetation LAI of evergreen needleleaf forests and evergreen broadleaf forests. Likewise, it is unrealistic that same values were set for field capacity of clay and sand.

It should be noted that four hydrological signatures could not be well simulated simultaneously in any individual sample from Sobol's sensitivity analysis. Hence, in order to obtain better model simulation, multi-objective calibration is necessary to achieve optimal parameter sets. Considering the complexity of model and large number of parameters, manual calibration is inefficient and difficult to obtain global optimal parameter sets. Automatic calibration is preferred for DHSVM with parallel computing to reduce computational burden. Traditional calibration is usually performed with a single objective (Guo *et al.* 2014, Wang and Brubaker 2015). However, a single objective is often inadequate to meet multiple requirements (Vrugt *et al.* 2003). Efficient global optimization algorithms are therefore recommended for use to reliably search for the global optimal parameter sets (Zhang *et al.* 2013, Ye *et al.* 2014).

Peak flow is slightly underestimated in the model simulation of DHSVM. The possible reasons for this are from various dimensions. Firstly, model structural problems related to peak flow generation mechanism may exist in DHSVM, including that preferential flow was not considered in this study and the assumption that understory vegetation (if it exist) covers the entire cell in evapotranspiration mode. Secondly, only limited meteorological stations and daily scale data are used in the study. According to Booij (2003, 2005), the spatial and temporal variability of precipitation will affect the hydrological simulation. As shown in the test application from Wigmosta *et al.* (1994), the best time step of meteorological data for model simulation is 3-hour. Additionally, determination of appropriate resolution of DEM may be critical for model simulation. According to Dubin and Lettenmaier (1999), simulations of peak flow and runoff process are greatly impacted by DEM resolution. Safeeq and Fares (2012) also concluded that underestimation of the peak flows exist when modeling runoff of a Hawaiian watershed.

5. Conclusion

In this study, a two-step sensitivity analysis approach was used. Firstly, the sensitivity of nearly all parameters in DHSVM which was built for Jinhua River Basin, East China, was roughly analyzed via ANOVA. Sobol's sensitivity analysis method, a variance-based global sensitivity analysis method, was then applied to analyze the contributions of the preliminary influential parameters identified by ANOVA to streamflow simulation, including single contributions, total contributions and interaction contributions. Parallel computing was applied to reduce the computational burden. For all samples from Sobol's sensitivity analysis, performances of hydrological signatures were also investigated. Additionally, peak flows extracted from the observation and simulation via POT approach were compared. The key findings of this study are summarized below:

(1) According to the Sobol's method, only a few number of model parameters are significantly sensitive in Jinhua River Basin, including a constant parameter (rain LAI multiplier), four soil parameters (lateral conductivity, porosity, field capacity and wilting point of clay loam), and three vegetation parameters (understory monthly LAI, understory minimum resistance and root zone depths of croplands). More attention should be paid to these parameters in future model calibration.

(2) The interactions between parameters cannot be ignored. For example, the total order sensitivity index of field capacity of clay loam reaches to 0.29, which is much larger than the first order sensitivity index (0.18) after considering the interactions between field capacity of clay loam and other parameters.

(3) High value of the objective function (*NE*) didn't indicate excellent performance of hydrological signatures. For most samples from Sobol's sensitivity analysis, water yield was simulated very well via DHSVM. However, minimum and maximum annual daily runoffs were underestimated in a majority of samples. And most of seven-day minimum runoffs were overestimated. However, good performances of these three signatures still exist in a number of samples.

(4) The model performances of specific individual samples in percentile analysis were summarized. Considering sensitive parameters together with their values, the good performance of maximum annual daily runoff in *Sample D* is owing to the low values of

rain LAI multiplier, understory monthly LAI and root zone depth. Likewise, *Sample PC* has the best performance in that its small, medium and large floods show less underestimation than others.

(5) Percentiles of peak flows extracted from the observed and simulated runoff indicate that small and medium floods were simulated reasonably. Slight underestimations happen to large floods. This is possibly due to the shortcomings of model structure and insufficient meteorological data used in the study.

(6) The work in this study helps further multi-objective calibration of DHSVM model and indicates where to improve to enhance the reliability and credibility of model simulation. Good simulation of the complete hydrograph is useful for water resources management, flood prediction and forecasting. Furthermore, the two-step sensitivity analysis approach can be applied to detailed parameter identification for model simulation with numerous parameters. The limitation of this approach lies in its demand for a large number of model runs.

Acknowledgements

National Climate Center of China Meteorological Administration, Zhejiang Provincial Metrological Administration and Zhejiang Provincial Hydrology Bureau are greatly acknowledged for providing meteorological and hydrological data used in this study. The valuable comments and suggestions from Editor and three anonymous reviewers are greatly appreciated.

Funding

This work was supported by National Natural Science Foundation of China (91547106 and 51379183), Zhejiang Provincial Natural Science Foundation of China (LR14E090001), and National Key Research and Development Plan "Inter-governmental Cooperation in International Scientific and Technological Innovation"(2016YFE0122100).

Disclosure statement

No potential conflict of interest was reported by the authors.

References

Andres, T.H., 1997. Sampling methods and sensitivity analysis for large parameter sets. *Journal of Statistical Computation and Simulation*, 57(1-4), 77-110. doi:10.1080/00949659708811804

Archer, D. and Newson, M., 2002. The use of indices of flow variability in assessing the hydrological and instream habitat impacts of upland afforestation and drainage. *Journal of Hydrology*, 268(1), 244-258. doi:10.1016/S0022-1694(02)00171-3

Bahremand, A. and De Smedt, F., 2008. Distributed hydrological modeling and sensitivity analysis inTorysa watershed, Slovakia. *Water Resources Management*, 22, 393-408. doi:10.1007/s11269-007-9168-x

Bittelli, M., et al., 2010. Development and testing of a physically based, three-dimensional model of surface and subsurface hydrology. *Advances in Water Resources*, 33(1), 106-122. doi:10.1016/j.advwatres.2009.10.013

Bois, B., et al., 2008. Using remotely sensed solar radiation data for reference evapotranspiration estimation at a daily time step. *Agricultural and Forest Meteorology*, 148(4): 619-630. doi:10.1016/j.agrformet.2007.11.005

Booij, M.J., 2003. Determination and integration of appropriate spatial scales for river basin modelling. *Hydrological Processes*, 17(13), 2581-2598. doi: 10.1002/hyp.1268

Booij, M.J., 2005. Impact of climate change on river flooding assessed with different spatial model resolutions. *Journal of Hydrology*, 303(1), 176-198. doi: 10.1002/hyp.1268

Bormann, H., Pinter, N., and Elfert, S., 2011. Hydrological signatures of flood trends on German rivers: Flood frequencies, flood heights and specific stages. *Journal of Hydrology*, 404(1), 50-66. doi:10.1016/j.jhydrol.2011.04.019

Cao, Q., et al., 2016. Climate and land cover effects on the temperature of Puget sound streams. *Hydrological Processes*, 30, 2286-2304. doi: 10.1002/hyp.10784

Chen, Y., Li, J., and Xu, H., 2016. Improving flood forecasting capability of physically based distributed hydrological models by parameter optimization. *Hydrology and Earth System Sciences*, 20(1), 375-392. doi:10.5194/hessd-12-10603-2015

Cibin, R., Sudheer, K.P., and Chaubey, I., 2010. Sensitivity and identifiability of stream flow generation parameters of the SWAT model. *Hydrological Processes*, 24(9), 1133-1148. doi: 10.1002/hyp.7568

Criss, R.E. and Winston, W.E., 2008. Do Nash values have value? Discussion and alternate proposals. *Hydrological Processes*, 22(14), 2723-2725. doi: 10.1002/hyp

Cuartas, L.A., et al., 2012. Distributed hydrological modeling of a micro-scale rainforest watershed in Amazonia: Model evaluation and advances in calibration using the new HAND terrain model. *Journal of Hydrology,* 462-463, 15-27. doi: http://dx.doi.org/10.1016/j.jhydrol.2011.12.047

Cuo, L., Giambelluca, T.W., and Ziegler, A.D., 2011. Lumped parameter sensitivity analysis of a distributed hydrological model within tropical and temperate catchments. *Hydrological Processes*, 25(15), 2405-2421. doi: 10.1002/hyp.8017

Domenico, P.A. and Schwartz, F.W., 1998. *Physical and chemical hydrogeology*. New York: Wiley.

Dubin, A.M. and Lettenmaier, D.P., 1999. Assessing the influence of digital elevation model resolution on hydrologic modeling. *University of Washington, Department of Civil and Environmental Engineering: Water Resources Series*, Technical Report No.159.

Du, E., et al., 2014. Validation and sensitivity test of the distributed hydrology soil-vegetation model (DHSVM) in a forested mountain watershed. *Hydrological Processes*, 28(26), 6196-6210. doi: 10.1002/hyp.10110

Du, J., et al., 2012. Assessing the effects of urbanization on annual runoff and flood events using an integrated hydrological modeling system for Qinhuai River basin, China. *Journal of Hydrology*, 464, 127-139. doi:10.1016/j.jhydrol.2012.06.057

Fisher, R.A., 1925. *Statistical methods for research workers*. New York: Springer.

Guo, J., et al., 2014. Multi-objective optimization of empirical hydrological model for streamflow prediction. *Journal of Hydrology*, 511, 242-253. doi:10.1016/j.jhydrol.2014.01.047

Gupta, H.V., Wagener, T., and Liu, Y., 2008. Reconciling theory with observations: elements of a diagnostic approach to model evaluation. *Hydrological Processes*, 22(18), 3802-3813. doi: 10.1002/hyp.6989

Hartmann, A., et al., 2013a. Testing the realism of model structures to identify karst system processes using water quality and quantity signatures. *Water Resources Research*, 49, 3345-3358, doi:10.1002/wrcr.20229

Hartmann, A., 2013b. Process-based karst modelling to relate hydrodynamic and hydrochemical characteristics to system properties. *Hydrology and Earth System Sciences,* 17(8), 3305-3321, doi:10.5194/hess-17-3305-2013

Hartmann, A., et al., 2015. A large-scale simulation model to assess karstic groundwater recharge over Europe and the Mediterranean. *Geoscientific Model Development,* 8(6): 1729-1746. doi:10.5194/gmd-8-1729-2015, 2015.

Hirsch, R.M. and Archfield, S.A., 2015. Flood trends: not higher but more often. *Nature Climate Change*, 5(3), 198-199. doi:10.1038/nclimate2551

Kelleher, C., Wagener, T., and McGlynn, B., 2015. Model-based analysis of the influence of catchment properties on hydrologic partitioning across five mountain headwater subcatchments. *Water Resources Research*, 51(6), 4109-4136. doi: 10.1002/2014WR016147

Krause, P., Boyle, D.P., and Bäse, F., 2005. Comparison of different efficiency criteria for hydrological model assessment. *Advances in Geosciences*, 5, 89-97. doi: 1680-7359/adgeo/2005-5-89

Lang, M., Ouarda, T.B.M.J., and Bobée, B., 1999. Towards operational guidelines for over-threshold modeling. *Journal of hydrology,* 225.3: 103-117. doi:http://dx.doi.org/10.1016/S0022-1694(99)00167-5

Lindman, H.R., 1974. *Analysis of Variance in Complex Experimental Designs*. San Francisco: W. H. Freeman & Co.

Mallakpour, I. and Villarini, G., 2015. The changing nature of flooding across the central United States. *Nature Climate Change*, 5(3), 250-254. doi:10.1038/nclimate2516

Moradkhani H and Sorooshian S., 2008. General review of rainfall-runoff modeling: model calibration, data assimilation, and uncertainty analysis. *Hydrological modelling and the water cycle*, 1-24.

Muleta, M., 2012. Model Performance Sensitivity to Objective Function during Automated Calibrations. *Journal of Hydrologic Engineering*, 17, 756-767. doi:10.1061/(ASCE)HE.1943-5584.0000497

Nash, J.E. and Sutcliffe, J.V., 1970. River flow forecasting through conceptual models. Part 1. A discussion of principles. *Journal of Hydrology*, 10, 282-290. doi:10.1016/0022-1694(70)90255-6

Noori, N. and Kalin, L., 2016. Coupling SWAT and ANN models for enhanced daily streamflow prediction. *Journal of Hydrology*, 533, 141-151. doi:10.1016/j.jhydrol.2015.11.050

Noori, N., Kalin, L., and Lockaby, G., 2014. Predicting impacts of changing land use/cover on streamflow in ungauged watersheds. *ASCE World Environmental & Water Resources Congress*, 1-5. doi: 10.1061/9780784413548.219

Obrien, E.J., et al., 2015. A review of probabilistic methods of assessment of load effects in bridges. *Structural Safety*, 53, 44-56. doi:10.1016/j.strusafe.2015.01.002

Olden, J.D. and Poff, N.L., 2003. Redundancy and the choice of hydrologic indices for characterizing streamflow regimes. *River Research and Applications*, 19(2), 101-121. doi: 10.1002/rra.700

Palanisamy, B. and Workman, S.R., 2014. Observed hydrographs: on their ability to infer a time-invariant hydrological transfer function for flow prediction in ungauged basins. *Hydrological Processes*, 28(3), 401-413. doi: 10.1002/hyp.9583

Pianosi, F., et al., 2016. Sensitivity analysis of environmental models: A systematic review with practical workflow, *Environmental Modelling & Software*, 79(MAY), 214-232. doi: 10.1016/j.envsoft.2016.02.008

Rahman, K., et al., 2013. Streamflow modeling in a highly managed mountainous glacier watershed using SWAT: the Upper Rhone River watershed case in Switzerland. *Water Resources Management*, 27(2), 323-339. doi:10.1007/s11269-012-0188-9

Rajabi, M.M., Ataie-Ashtiani, B., and Simmons, C.T., 2015. Polynomial chaos expansions for uncertainty propagation and moment independent sensitivity analysis of seawater intrusion simulations. *Journal of Hydrology*, 520, 101-122. doi:10.1016/j.jhydrol.2014.11.020

Rao, A.R. and Han, J., 1987. Analysis of objective functions used in urban runoff models. *Advances in Water Resources*, 10(4), 205-211. doi:10.1016/0309-1708(87)90030-3

Raposo, J.R., Molinero, J., and Dafonte, J., 2012. Parameterization and quantification of recharge in crystalline fractured bedrocks in Galicia-Costa (NW Spain). *Hydrology and Earth System Sciences*, 16(6), 1667-1683. doi:10.5194/hess-16-1667-2012

Razavi, T. and Coulibaly, P., 2012. Streamflow prediction in ungauged basins: review of regionalization methods. *Journal of Hydrologic Engineering*, 18(8), 958-975. doi: 10.1061/(ASCE)HE.1943-5584.0000690

Ren, H., et al., 2016. Classification of hydrological parameter sensitivity and evaluation of parameter transferability across 431 US MOPEX basins. *Journal of Hydrology*, 536, 92-108. doi:10.1016/j.jhydrol.2016.02.042

Safeeq, M. and Fares, A., 2012. Hydrologic response of a Hawaiian watershed to future climate change scenarios. *Hydrological Processes*, 26(18), 2745-2764. doi: 10.1002/hyp.8328

Saltelli, A., et al., 2004. *Sensitivity analysis in practice: a guide to assessing scientific models*. New York: Wiley.

Saltelli, A., Andres, T.H., and Homma, T., 1995. Sensitivity analysis of model output, Performance of the iterated fractional factorial design method. *Computational Statistics & Data Analysis*, 20, 387-407. doi:10.1016/0167-9473(95)92843-M

Saltelli, A., Chan, K., and Scott, E.M., 2000a. *Sensitivity Analysis*. New York: Wiley,.

Saltelli, A., and Tarantola, S., 2002. On the relative importance of input factors in mathematical models: safety assessment for nuclear waste disposal. *Journal of the American Statistical Association*, 97(459), 702-709. http://dx.doi.org/10.1198/016214502388618447

Saltelli, A., Tarantola, S., and Campolongo, F., 2000b. Sensitivity analysis as an ingredient of modeling. *Statistical Science*, 377-395. DOI: 10.1214/ss/1009213004

Sawicz, K., et al., 2011. Catchment classification: empirical analysis of hydrologic similarity based on catchment function in the eastern USA. *Hydrology and Earth System Sciences*, 15(9), 2895-2911. doi:10.5194/hess-15-2895-2011

Schaefli, B. and Gupta, H.V., 2007. Do Nash values have value? *Hydrological Processes*, 21(15), 2075-2080. doi: 10.1002/hyp.6825

Shafii, M. and Tolson, B.A., 2015. Optimizing hydrological consistency by incorporating hydrological signatures into model calibration objectives. *Water Resources Research*, 51(5), 3796-3814. doi: 10.1002/2014WR016520

Shinohara, Y., et al., 2016. Effects of plant roots on the soil erosion rate under simulated rainfall with high kinetic energy. *Hydrological Sciences Journal*, 61:13, 2435-2442, doi:10.1080/02626667.2015.1112904

Sobol', I.M., 2001. Global sensitivity indices for nonlinear mathematical models and their Monte Carlo estimates. *Mathematics and Computers in Simulation*, 55(1-3), 271-280. doi:10.1016/S0378-4754(00)00270-6

Song, X., et al., 2015. Global sensitivity analysis in hydrological modeling: Review of concepts, methods, theoretical framework, and applications. *Journal of Hydrology*, 523, 739-757. doi:10.1016/j.jhydrol.2015.02.013

Steel, R.G.D. and Torrie, J.H., 1988. *Principles and Procedures of Statistics*. 2nd ed. New York: McGraw Hill.

Surfleet, C.G., Skaugset, A.E., and McDonnell, J.J., 2010. Uncertainty assessment of forest road modeling with the Distributed Hydrology Soil Vegetation Model (DHSVM). *Canadian Journal of Forest Research*, 40(7), 1397-1409. doi:10.1139/X10-079

Tan, M.L., et al., 2015. Impacts of land-use and climate variability on hydrological components in the Johor River basin, Malaysia. *Hydrological Sciences Journal*, 60:5, 873-889. doi:10.1080/02626667.2014.967246

Tang, Y., et al., 2007a. Advancing the identification and evaluation of distributed rainfall-runoff models using global sensitivity analysis. *Water Resources Research*, 43(6). doi: 10.1029/2006WR005813

Tang, Y., et al., 2007b. Comparing sensitivity analysis methods to advance lumped watershed model identification and evaluation. *Hydrology and Earth System Sciences Discussions*, 11(2), 793-817. doi:10.5194/hess-11-793-2007

Thanapakpawin, P., et al., 2007. Effects of land use change on the hydrologic regime of the Mae Chaem river basin, NW Thailand. *Journal of Hydrology*, 334(1-2), 215-230. doi: http://dx.doi.org/10.1016/j.jhydrol.2006.10.012

Vrugt, J.A., et al., 2003. Effective and efficient algorithm for multiobjective optimization of hydrologic models. *Water Resources Research*, 39(8). doi: 10.1029/2002WR001746

Wagener, T., et al., 2001. A frame-work for development and application of hydrological models, *Hydrology and Earth System Sciences Discussion*, 5(1): 13-26. doi:10.5194/hess-5-13-2001, 2001.

Wagener, T., et al., 2007. Catchment classification and hydrologic similarity. *Geography Compass*, 1(4), 901-931. doi: 10.1111/j.1749-8198.2007.00039.x

Wang, Y. and Brubaker, K., 2015. Multi-objective model auto-calibration and reduced parameterization: Exploiting gradient-based optimization tool for a hydrologic model. *Environmental Modelling & Software*, 70, 1-15. doi:10.1016/j.envsoft.2015.04.001

Westerberg, I.K. and McMillan, H.K., 2015. Uncertainty in hydrological signatures. *Hydrology and Earth System Sciences*, 19(9), 3951-3968. doi:10.5194/hess-19-3951-2015

Wigmosta, M.S. and Burges, S.J., 1997. An adaptive modeling and monitoring approach to describe the hydrologic behavior of small catchments. *Journal of Hydrology*, 202(1), 48-77. doi:10.1016/S0022-1694(97)00057-7

Wigmosta, M.S., et al., 2002. The distributed hydrology soil vegetation model. *Mathematical models of small watershed hydrology and applications*, 7-42.

Wigmosta, M.S. and Lettenmaier, D.P., 1999. A comparison of simplified methods for routing topographically driven subsurface flow. *Water Resources Research*, 35(1), 255-264. doi: 10.1029/1998WR900017

Wigmosta, M.S. and Perkins, W.A., 2011. Simulating the effects of forest roads on watershed hydrology. *Land use and watersheds: human influence on hydrology and geomorphology in urban and forest areas* 127-143. doi: 10.1029/WS002p0127

Wigmosta, M.S., Vail, L.W., and Lettenmaier, D.P., 1994. A distributed hydrology-vegetation model for complex terrain. *Water Resources Research*, 30(6), 1665-1679. doi: 10.1029/94WR00436

Winchell, M.F., et al., 2015. Using SWAT for sub-field identification of phosphorus critical source areas in a saturation excess runoff region. *Hydrological Sciences Journal*, 60:5, 844-862. doi: 0.1080/02626667.2014.980262

Winsemius, H.C., et al., 2009. On the calibration of hydrological models in ungauged basins: A framework for integrating hard and soft hydrological information. *Water Resources Research*, 45(12). doi: 10.1029/2009WR007706

Xu, Y. and Mynett, A.E., 2006. Application of uncertainty and sensitivity analysis in river basin management. *Water Science and Technology*, 53(1), 41-49. doi: 10.2166/wst.2006.006

Xu, Y.P., et al., 2015. Coupling a Regional Climate Model and a Distributed Hydrological Model to Assess Future Water Resources in Jinhua River Basin, East China. *Journal of Hydrologic Engineering*, 20(4), 04014054. doi: 10.1061/(ASCE)HE.1943-5584.0001007

Xu, Y.P., et al., 2014. Future potential evapotranspiration changes and contribution analysis in Zhejiang Province, East China. *Journal of Geophysical Research-Atmospheres*, 119(5), 2174-2192. doi: 10.1002/2013JD021245

Xu, Y.P., et al., 2013. Impact of climate change on hydrology of upper reaches of Qiantang River Basin, East China. *Journal of Hydrology*, 483, 51-60. doi:10.1016/j.jhydrol.2013.01.004

Yadav, M., Wagener, T., and Gupta, H., 2007. Regionalization of constraints on expected watershed response behavior for improved predictions in ungauged basins. *Advances in Water Resources*, 30(8), 1756-1774. doi:10.1016/j.advwatres.2007.01.005

Yan. J. and Haan, C.T., 1991. Mutiobjective Parameter estimation for hydrologic models-Weighting of errors. *Transactions of the ASAE*, 34(1), 135-141. doi: 10.13031/2013.31635

Ye, L., et al., 2014. Multi-objective optimization for construction of prediction interval of hydrological models based on ensemble simulations. *Journal of Hydrology*, 519, 925-933. doi:10.1016/j.jhydrol.2014.08.026

Yilmaz, K.K., Gupta, H.V., and Wagener, T., 2008. A process-based diagnostic approach to model evaluation: Application to the NWS distributed hydrologic model. *Water Resources Research*, 44(9). doi: 10.1029/2007WR006716

Zhan, C.S., et al., 2013. An efficient integrated approach for global sensitivity analysis of hydrological model parameters. *Environmental Modelling & Software*, 41, 39-52. doi:10.1016/j.envsoft.2012.10.009

Zhang, C., Chu, J., and Fu, G., 2013. Sobol′'s sensitivity analysis for a distributed hydrological model of Yichun River Basin, China. *Journal of Hydrology*, 480, 58-68. doi:10.1016/j.jhydrol.2012.12.005

Zhang, X., et al., 2013. Efficient multi-objective calibration of a computationally intensive hydrologic model with parallel computing software in Python. *Environmental Modelling & Software*, 46, 208-218. doi:10.1016/j.envsoft.2013.03.013

Table 1. Vegetation and soil classes and their percentages in Jinhua River Basin.

Table 2. Ranges, unit and abbreviation of constant, soil and vegetation parameters for ANOVA sensitivity analysis.

Table 3. Description of the six hydrological signatures used in the study.

Table 4. Ranges, number and abbreviation of parameters for Sobol's sensitivity analysis.

Table 5. Selected samples based on the *NE* value.

Table 6. Hydrological signatures of the observed and the simulated from selected samples and corresponding *P*-values.

Table 7. Selected samples for peak flow based on the *NS* value.

Figure 1. Methodology framework used in this study.

Figure 2. Location of the six stations used in the study.

Figure 3. DEM (digital elevation map) (a) soil distribution (b) and vegetation distribution (c) in Jinhua River Basin.

Figure 4. ANOVA parameter sensitivities based on the *NE* measure (*F*-value > 3).

Figure 5. Model performance in 1994, 1995 and 1996 (corresponding to moderate, wet and dry year, respectively) when the value of *NE* (*NS*, E_{rel} and *NE* are 0.83, 0.81 and 0.82 respectively) is the maximum in ANOVA sensitivity analysis.

Figure 6. Sobol's total order sensitivity index based on the *NE* measure.

Figure 7. Interactions among sixteen parameters based on the *NE* measure.

Figure 8. Boxplot for *P*-value of hydrological signatures (A1 (Mean annual runoff), L1 (Low flow signature), L2 (Base-flow signature): and H1 (Specific mean annual maximum flows)) of all samples in Sobol's sensitivity analysis.

Figure 9. Hydrological signature *DH1-4* for observed and simulated runoff from four selected samples as shown in Table 5.

Figure 10. Hydrological signature *DL1-4* for observed and simulated runoff from four selected samples as shown in Table 5.

Figure 11. Peak flow percentiles for observed and simulated runoff from samples whose *NE* > 0.7 in Sobol's sensitivity analysis.

Figure 12. Peak flow percentiles for observed and simulated runoff from three selected samples as shown in Table 7.

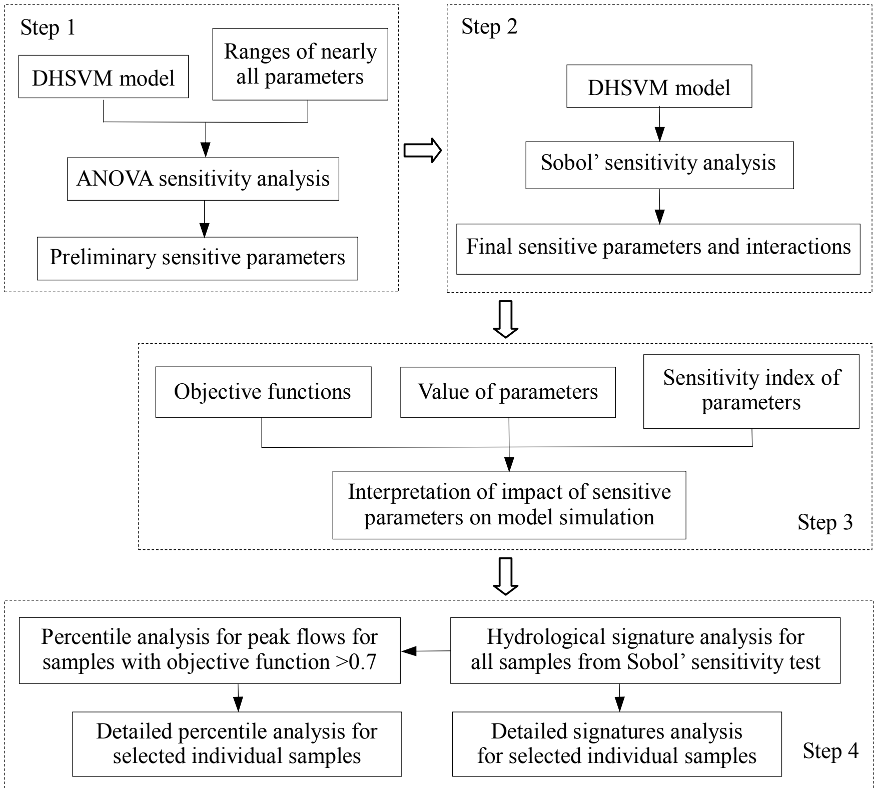

Figure 1. Methodology framework used in this study.

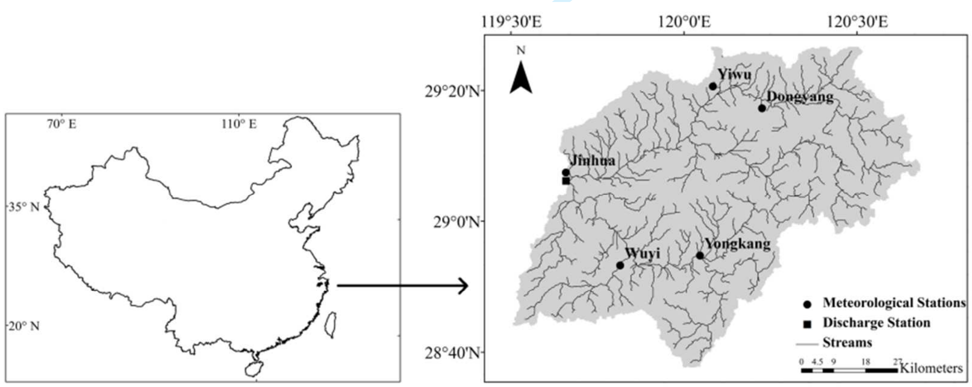

Figure 2. Location of the six stations used in the study.

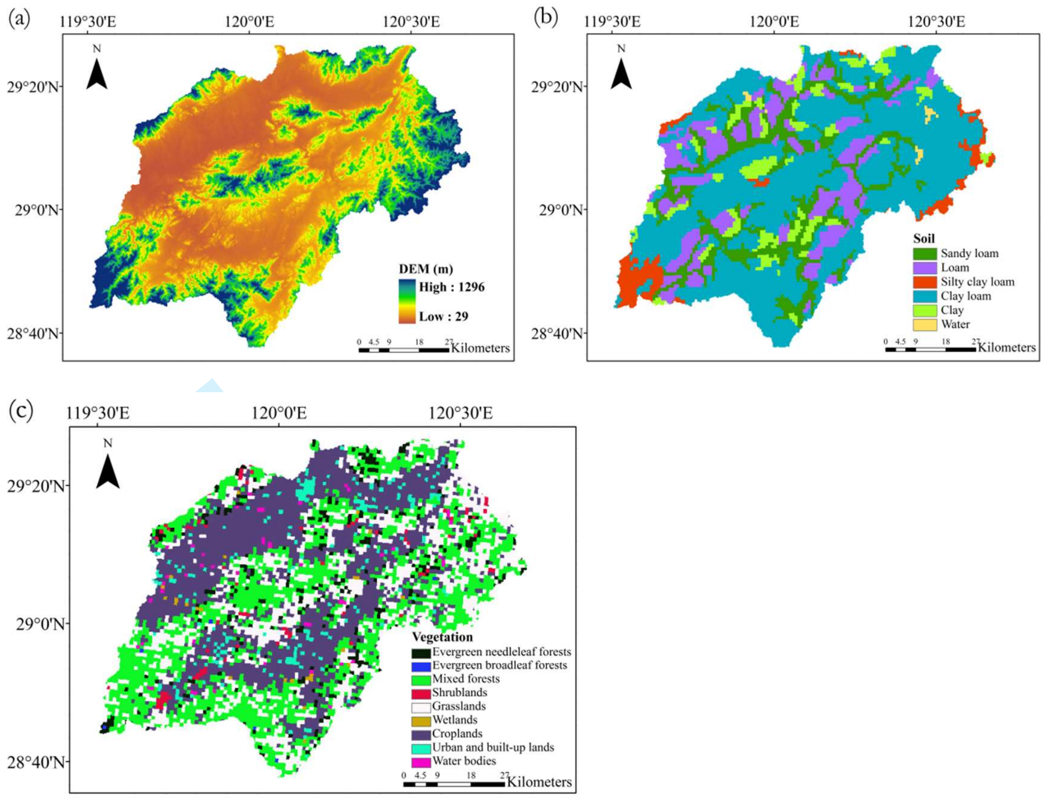

Figure 3. DEM (digital elevation map) (a) soil distribution (b) and vegetation distribution (c) in Jinhua River Basin.

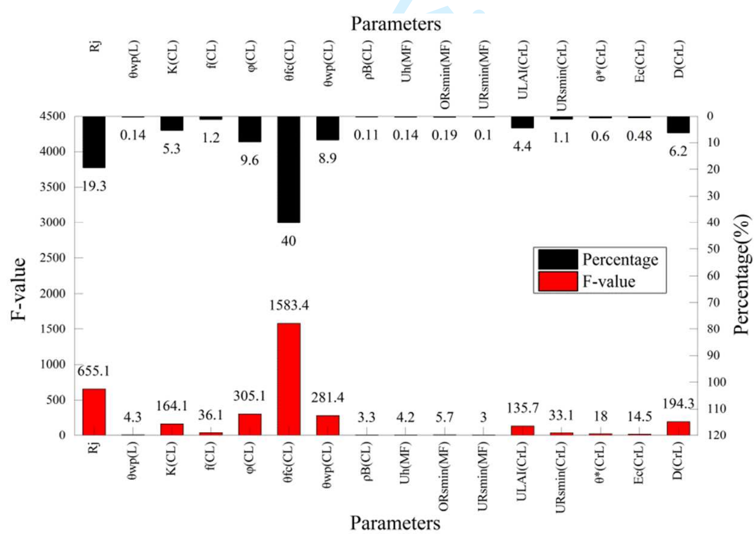

Figure 4. ANOVA parameter sensitivities based on the *NE* measure (F-value > 3).

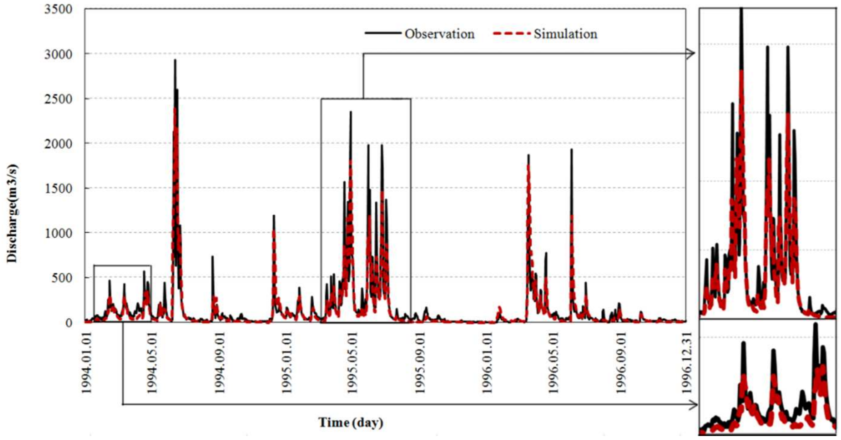

Figure 5. Model performance in 1994, 1995 and 1996 (corresponding to moderate, wet and dry year, respectively) when the value of *NE* (*NS*, *E*rel and *NE* are 0.83, 0.81 and 0.82 respectively) is the maximum in ANOVA sensitivity analysis.

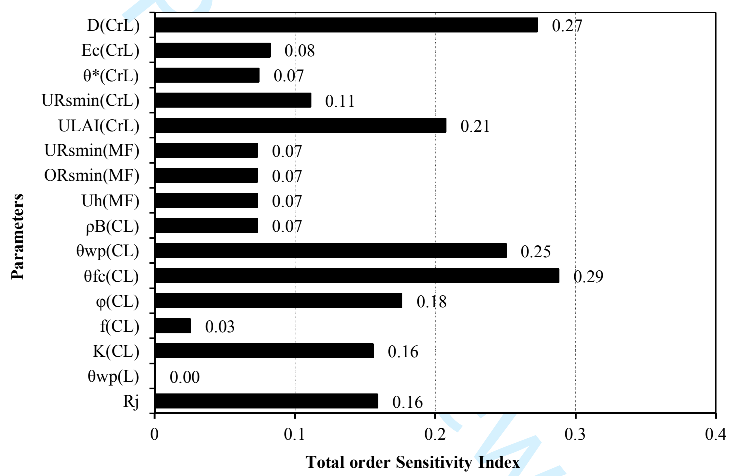

Figure 6. Sobol's total order sensitivity index based on the *NE* measure.

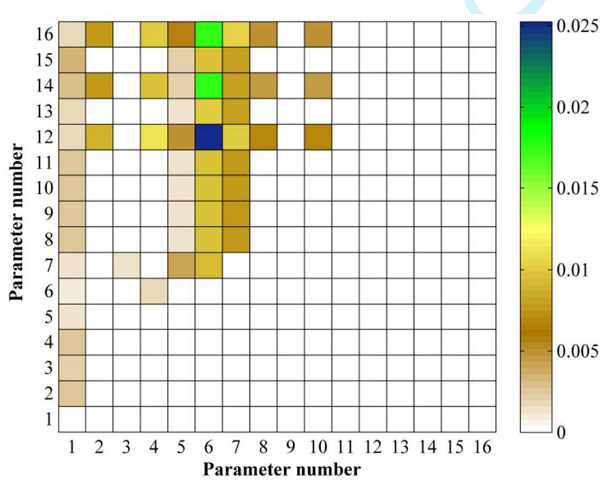

Figure 7. Interactions among sixteen parameters based on the *NE* measure.

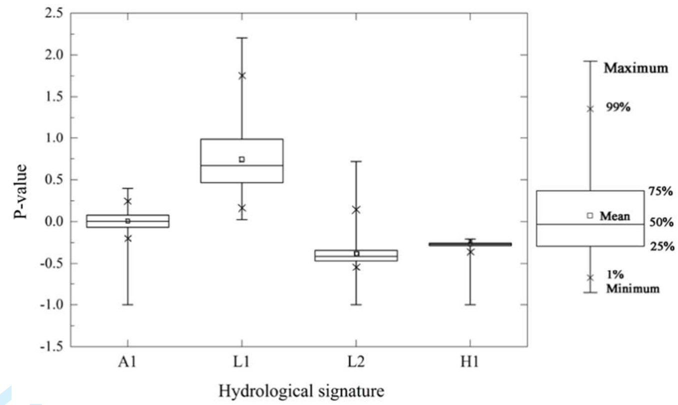

Figure 8. Boxplot for *P*-value of hydrological signatures (A1 (Mean annual runoff), L1 (Low flow signature), L2 (Base-flow signature): and H1 (Specific mean annual maximum flows)) of all samples in Sobol's sensitivity analysis.

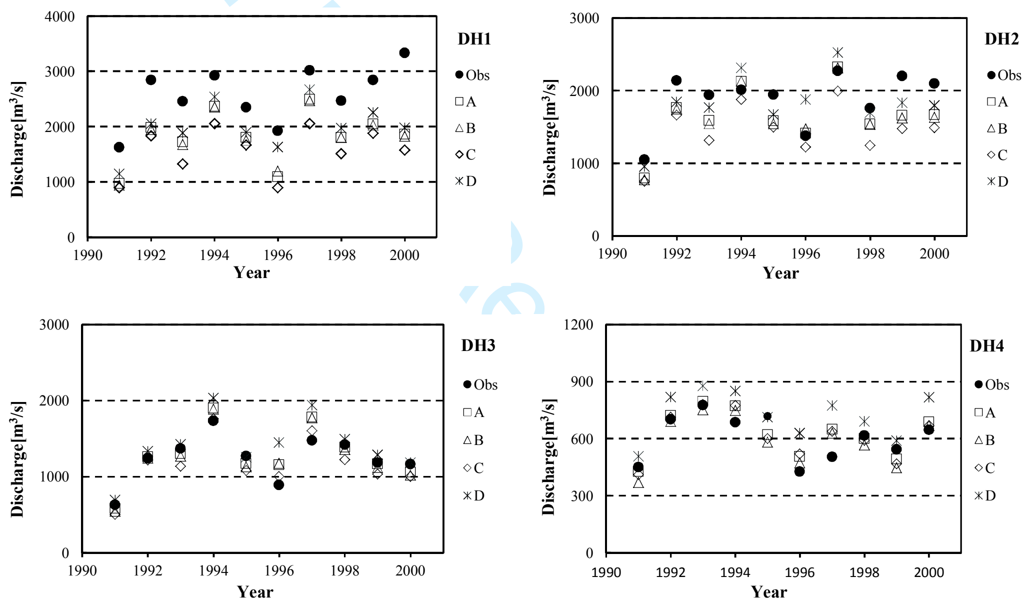

Figure 9. Hydrological signatures *DH1-4* for observed and simulated runoff from four selected samples as shown in Table 5.

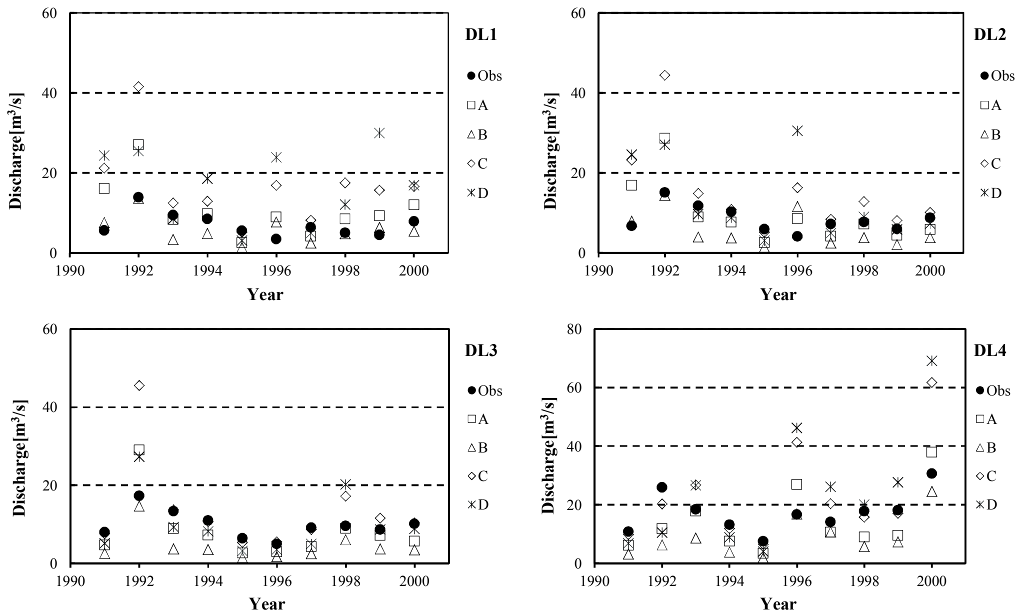

Figure 10. Hydrological signature *DL1-4* for observed and simulated runoff from four selected samples as shown in Table 5.

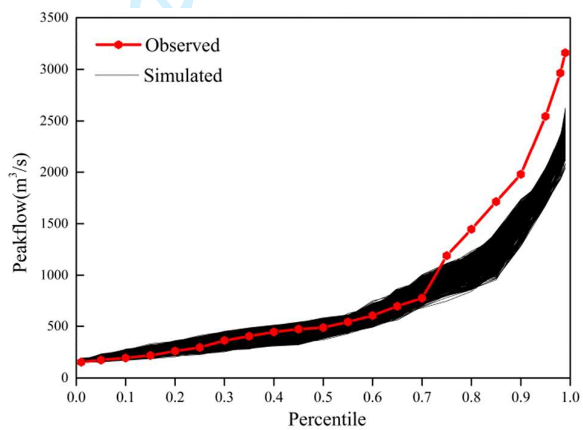

Figure 11. Peak flow percentiles for observed and simulated runoff from samples whose NS > 0.7 in Sobol's sensitivity analysis.

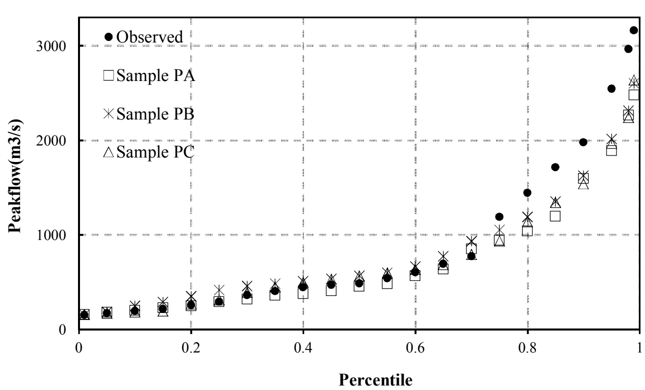

Figure 12. Peak flow percentiles for observed and simulated runoff from three selected samples as shown in Table 7.

Table 1. Vegetation and soil classes and their percentages in Jinhua River Basin.

Vegetation	Percentages	Vegetation	Percentages
Evergreen needleleaf forests	5.0	Water bodies	0.8
Evergreen broadleaf forests	0.1	**Soil**	**Percentages**
Mixed forests	*29.6*	*Sandy loam*	*16.5*
Shrublands	1.2	*Loam*	*15.8*
Grasslands	*22.9*	Silty clay loam	4.6
Wetlands	0.4	*Clay loam*	*55.4*
Croplands	*36.7*	Clay	7.3
Urban and built-up lands	3.3	Water	0.4

The italics represent soil/vegetation types whose area percentages are bigger than 10%.

Table 2. Ranges, unit and abbreviation of constant, soil and vegetation parameters for ANOVA sensitivity analysis.

Parameters	Abbrev.	Range	Parameters	Abbrev.	Range
Constant Parameters			**Vegetation Parameters(Grasslands, GL; Croplands, CrL)**		
Ground Roughness(m)	Zou	0.001~0.03	Understory Root Fraction	UFrjk	0~1
Rain Threshold(□)	Tmin	-1~0	Understory Monthly LAI(m^2/m^2)	ULAI	0.3~3
Reference Height(m)	Zr	30~50	Understory Monthly Alb	Uαj	0.1~0.3
Rain LAI Multiplier(m)	Rj	0.00001~0.001	Understory Height(m)	Uh	0.3~2.5
Temperature Lapse Rate(□/m)	Lt	-0.008~ 0	Maximum Resistance(s/m)	Rsmax	300~1000
Vegetation Parameters(Mixed Forest, MF)			Understory Minimum Resistance(s/m)	URsmin	50~300
Fractional Coverage (m^2/m^2)	F	0.7~1	Soil Moisture Threshold(m^3/m^3)	θ^*	0.1~0.35
Radiation Attenuation	Lb	0.1~0.3	Vapor Pressure Deficit(pa)	Ec	1000~6000
Trunk Space(m/m)	Rt	0.4~0.6	Rpc	Rpc	10~50
Aerodynamic Attenuation	Na	1.5~3.5	Root Zone Depths(m)	D	0.1~0.8
Overstory Root Fraction	OFrjk	0~1	**Soil Parameters(Sandy Loam, SL; Loam, L; Clay Loam, CL)**		
Overstory Monthly LAI(m^2/m^2)	OLAI	5~10	Lateral Conductivity (m/s)	K	0.00001~0.09
Overstory Monthly Alb	Oαj	0.1~0.3	Lateral Conductivity Exponential Decrease	f	1~4
Understory Root Fraction	Ufrjk	0~1	Maximum Infiltration Rate (m/s)	Imax	0.00001~0.09
Understory Monthly LAI(m^2/m^2)	ULAI	0.3~3	Surface Albedo (m/s)	α	0.1~0.3
Understory Monthly Alb	Uαj	0.1~0.3	Porosity(m^3/m^3)	φ	0.35~0.6
Overstory Height(m)	*Oh*	*10~25*	Pore Size Distribution	m	0.2~0.5
Understory Height(m)	*Uh*	*0.3~2.5*	Bubbling Pressure(m)	Ψb	0.1~0.76
Maximum Resistance(s/m)	Rsmax	2000~7000	Field Capacity(m^3/m^3)	θfc	0.16~0.4
Overstory Minimum Resistance(s/m)	*ORsmin*	*300~800*	Wilting Point(m^3/m^3)	θwp	0.05~0.25
Understory Minimum Resistance(s/m)	*URsmin*	*50~300*	Bulk Density(kg/ m^3)	ρB	1000~3000
Moisture Threshold(m^3/m^3)	θ^*	0.1~0.35	Vertical Conductivity(m/s)	Ks	0.0001~0.5
Vapor Pressure Deficit(pa)	Ec	1000~60000	Thermal Conductivity (W/mK)	Kt	3~8
Rpc	Rpc	10~50	Thermal Capacity (J/m^3K)	CV	1×10^6~ 5×10^6
Root Zone Depths(m)	D	0.1~0.8			

The abbreviations SL, L and CL in Table 2 represent sandy loam, loam and clay loam respectively. Similarly, MF, GL and CrL represent mixed forests, grasslands and croplands respectively. The italics represent parameters whose ranges for two vegetation stories are set separately.

Table 3. Description of the six hydrological signatures used in the study.

Conditions	Hydrological signature	Abbrev.	Unit	Definition
Average flow conditions	Mean annual runoff	*A1*	$m^3s^{-1}km^{-2}$	Mean annual flow divided by catchment area
Low flow conditions	Low flow signature	*L1*	dimensionless	Mean of the lowest annual daily flow divided by mean annual daily flow averaged across all years
	Base-flow signature	*L2*	dimensionless	Seven-day minimum flow Divided by mean annual daily flows averaged across all years
Peak flow conditions	Specific mean annual maximum flows	*H1*	$m^3s^{-1}km^{-2}$	Mean annual maximum flows divided by catchment area
Duration of flow events: Low flow conditions	Annual minimum of 1-/3-/7-/30-day means of daily runoff	*DL1-4*	m^3s^{-1}	Magnitude of minimum annual flow of various duration, ranging from daily to monthly
Duration of flow events: Peak flow conditions	Annual maximum of 1-/3-/7-/30-day means of daily runoff	*DH1-4*	m^3s^{-1}	Magnitude of maximum annual flow of various duration, ranging from daily to monthly

Table 4. Ranges, number and abbreviation of parameters for Sobol's sensitivity analysis.

Number	Parameters	Abbrev.	Ranges	Number	Parameters	Abbrev.	Ranges
1	Rain LAI Multiplier	Rj	0.00001~0.00	9	Understory Height(MF)	Uh(MF)	0.3~2.5
2	Wilting Point(L)	θwp(L)	0.05~0.25	10	Overstory Minimum Resistance(MF)	ORsmin(MF)	300~800
3	Lateral Conductivity(CL)	K(CL)	0.00001~0.09	11	Understory Minimum Resistance(MF)	URsmin(MF)	50~300
4	Lateral (CL)	f(CL)	1~4	12	Understory Monthly LAI(CrL)	ULAI(CrL)	0.3~3
5	*Porosity(CL)*	*φ(CL)*	*0.35~0.6*	13	Understory Minimum Resistance(CrL)	URsmin(CrL)	50~300
6	*Field Capacity(CL)*	*θfc(CL)*	*0.16~0.4*	14	Soil Moisture Threshold(CrL)	θ^*(CrL)	0.1~0.35
7	*Wilting Point(CL)*	*θwp(CL)*	*0.05~0.25*	15	Vapor Pressure Deficit(CrL)	Ec(CrL)	1000~6000
8	Bulk Density(CL)	ρB(CL)	1000~3000	16	Root Zone Depths(CrL)	D(CrL)	0.1~0.8

The italics represent parameters in the Sobol's sensitivity analysis whose ranges differ from ANOVA.

Table 5. Selected samples based on the *NE* value.

NE	0.85-0.88	0.80-0.85	0.75-0.80	0.70-0.75
Sample	Sample A(max NE)	Sample B	Sample C	Sample D

Table 6. Hydrological signatures of the observed and the simulated from selected samples and corresponding *P*-values.

Hydrological Signature	Obs	Sample A		Sample B		Sample C		Sample D	
		Sim	P	Sim	P	Sim	P	Sim	P
A1	9.34	8.44	-0.10	7.17	-0.23	9.43	0.01	11.3	0.21
L1	0.05	0.08	0.68	0.05	0.07	0.11	1.37	0.092	0.97
L2	0.23	0.15	-0.35	0.11	-0.54	0.25	0.09	0.13	-0.42
H1	0.44	0.31	-0.29	0.31	-0.30	0.27	-0.39	0.34	-0.22

Table 7. Selected samples for peak flow based on the *NS* value.

NS	0.80-0.85	0.75-0.80	0.70-0.75
Sample	Sample PA (max NS)	Sample PB	Sample PC